Rotation velocities in the plasma edge driven viscously by scrape-off layer flows

W. M. Stacey
Georgia Institute of Technology, Atlanta, Georgia 30332, USA

(Received 15 April 2009; accepted 1 June 2009; published online 25 June 2009)

Scrape-off layer parallel flows and the viscous fluxes in the plasma edge driven thereby are calculated from neoclassical theory for a model problem representative of a present experiment, using an analytical model for elongated flux surface geometry with a Shafranov shift to provide a realistic evaluation of important poloidal dependences. The estimated effects of the viscous torques of toroidal and poloidal momentum driven by these scrape-off layer flows on rotation velocities in the edge plasma are substantial, suggesting possible explanations for various experimental observations. © *2009 American Institute of Physics*. [DOI: 10.1063/1.3158564]

I. INTRODUCTION

Recent probe measurements[1,2] of deuterium parallel flows in the scrape-off layer (SOL) of tokamaks have identified the presence of large magnitude flows with unanticipated variations between positive and negative parallel (poloidal) flows. Subsequent analyses have attributed these flow patterns to enhanced ballooning mode transport from the core into the outboard SOL,[1] to Pfirsch–Schluter flows from the core into the SOL,[3] to grad-B and curvature drifts between the core and SOL plasmas,[2,4] and to geometric flux surface compression-expansion effects on the poloidal distribution of the particle flux from the core into the SOL.[5] Independent of their cause, the existence of these large, poloidally nonuniform SOL flows must have an effect on the poloidal and toroidal rotation velocities just across the separatrix in the edge pedestal, and thus[6] on the structure of the density and radial electric field profiles in the edge pedestal.

The purpose of this paper is to describe a theoretical/computational investigation of the transfer of momentum between the SOL and the pedestal for a model problem with parameters representative of the DIII-D tokamak.[7] The flows along the separatrix were first calculated, taking into account grad-B and curvature drifts and geometric flux surface compression/expansion effects[4,5] on the outflow of particles and energy from the core into the SOL, but neglecting any transfer of momentum between the SOL and pedestal. Then the momentum transport across the separatrix that would be associated with such flows along the separatrix was calculated, and an estimate was made of a significant effect on the rotation velocities within the edge pedestal of such flows.

II. CALCULATION OF DEUTERIUM ION FLOW VELOCITIES IN THE SOL

First, average radial particle and power flows from the core into the SOL were calculated with an integrated modeling code[8] consisting of global power and particle balances on the core (taking into account neutral beam heating/fueling, neutral particle recycling, and radiative power losses), a "two-point" integrated model calculation of the particle and power fluxes incident on the divertor target plates, and a two-dimensional calculation of the neutral particles recycling from the divertor plate back into the divertor-SOL plasma and the core plasma. These average radial particle and power fluxes from the core into the SOL were then distributed poloidally, taking into account grad-B and curvature drifts and geometric flux surface compression/expansion, and input to a one-dimensional divertor model[4,5] to calculate densities, temperatures, electrostatic potential, parallel flow velocities, etc., along the separatrix from the inner to the outer divertor target plates.

Parallel deuterium particle velocities in the SOL calculated for a model problem representative of a DIII-D, lower single null (LSN) divertor, *H* (high)-mode discharge are shown in Fig. 1. The model problem geometry is indicated in Fig. 2, where the poloidal location of the various numbered regions referred to in Fig. 1 (and in subsequent figures) is shown. Two otherwise identical calculations were made, one with the toroidal field antiparallel to the plasma current (as shown in Fig. 2)—designated as $(B-)$—and a second calculation with the toroidal field reversed to be parallel to the plasma current—designated as $(B+)$. The $(B-)$ configuration produces grad-B and curvature drifts downward toward the LSN divertor, while the $(B+)$ configuration produces grad-B and curvatures drifts upward away from the LSN divertor. The effect of this difference in drifts on ion flow distributions between the plasma core and SOL is the primary reason for the differences in parallel velocity profiles shown in Fig. 1, as discussed in Ref. 4.

These parallel flows are decomposed into poloidal and toroidal rotation components in Figs. 3 and 4. The sign convention used for the rotation velocities is that the positive φ-direction is the direction of the plasma current and the positive θ-direction is in the right-hand sense with respect to the plasma current (i.e., in the direction which the fingers of the right hand wrap when the thumb is in the direction of the current—downward at the outboard midplane).

 © 2009 American Institute of Physics

Downloaded 06 Jan 2010 to 130.207.50.192. Redistribution subject to AIP license or copyright; see http://pop.aip.org/pop/copyright.jsp

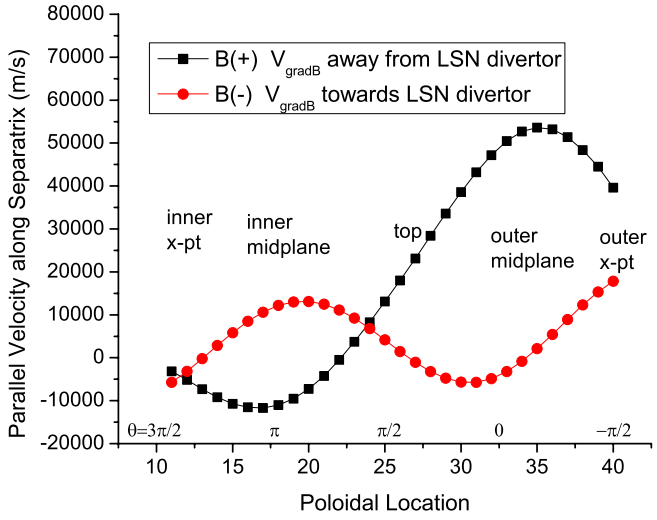

FIG. 1. (Color online) Parallel flow along separatrix.

III. CALCULATION OF MOMENTUM TRANSPORT ACROSS THE SEPARATRIX

A. Convection

A net radial ion flow from the core into the SOL was calculated from core particle balance, taking into account neutral beam fueling and neutral particle recycling. In terms of this $\Gamma_r^{\rm sep}=n^{\rm sep}V_r^{\rm sep}$, the ion x-momentum convection from the pedestal across the separatrix into the SOL is $m\Gamma_r^{\rm sep}V_x$, where $x=\varphi,\theta$ denotes toroidal or poloidal momentum, respectively. The calculated value of the radial particle flux at the separatrix was $V_r^{\rm sep}=23.7$ m/s, which together with the calculated values of $V_{\varphi,\theta}$ shown in Figs. 3 and 4, were used to evaluate this expression. Note that the positive sense of the parallel velocity is in the direction along the field lines from the inner to the outer divertor targets, which is in the positive toroidal direction for $(B+)$ but in the negative toroidal direction for $(B-)$. This results in the positive senses of the parallel and toroidal velocities being aligned for $(B+)$ but opposite for $(B-)$. The positive and negative senses of the poloidal and parallel velocities were aligned for both the $(B+)$ and $(B-)$ field directions.

B. Viscosity

Neoclassical theory yields the following expressions for the leading order radial fluxes of toroidal and poloidal momentum in generalized $(r-\theta-\varphi)$ geometry with axial symmetry[9] within the edge pedestal inside the separatrix

$$\Pi_{r\varphi}=-\eta_4 R\frac{\partial(V_\varphi R^{-1})}{h_\theta\partial\theta}, \tag{1}$$

$$\Pi_{r\theta}=-\frac{1}{2}\eta_4\left[(RB_\theta)^{-1}\frac{\partial(RB_\theta V_\theta)}{h_\theta\partial\theta}+R\frac{\partial(V_\varphi R^{-1})}{h_\theta\partial\theta}\right], \tag{2}$$

where $\eta_4=nT/\Omega=nT/(ZeB/m)$.

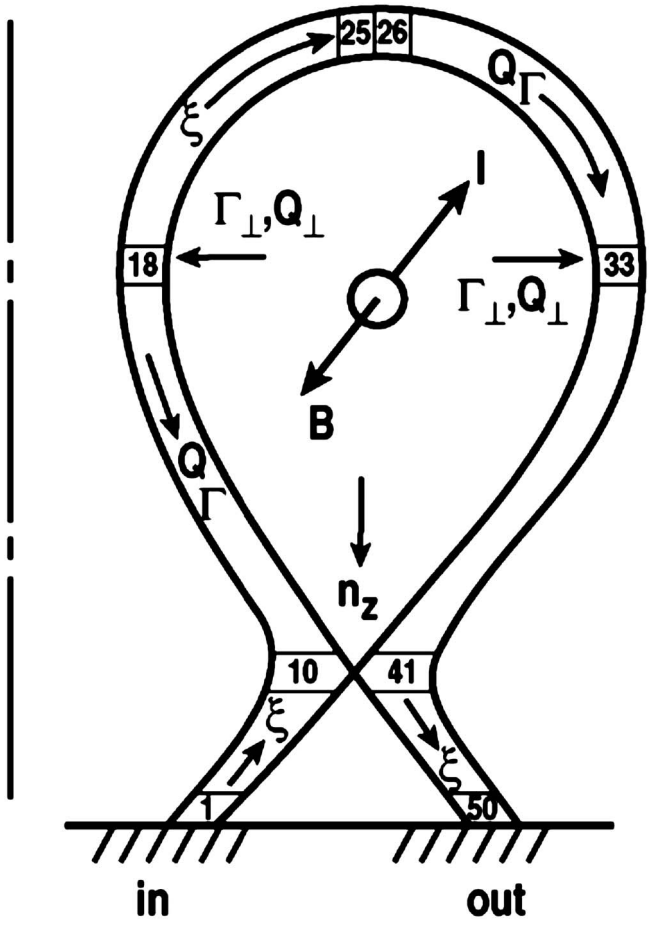

FIG. 2. Geometric SOL-divertor model (reprinted from Ref. 5).

C. Miller flux surface geometry

Since the above expressions for the leading order neoclassical viscosity inside the separatrix depend on the poloidal variation of the geometry, magnetic field and velocity, we use the analytical solution of Miller *et al.*[10] of the Grad–Shafranov equation in order to obtain an accurate represen-

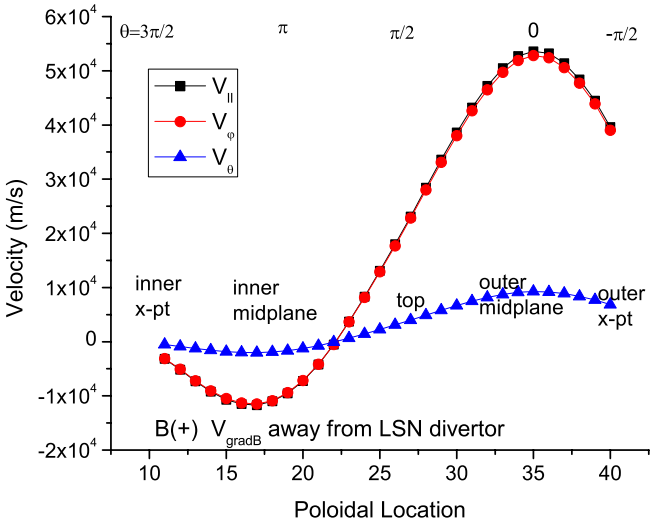

FIG. 3. (Color online) Velocities for $(B+)$ case.

Downloaded 06 Jan 2010 to 130.207.50.192. Redistribution subject to AIP license or copyright; see http://pop.aip.org/pop/copyright.jsp

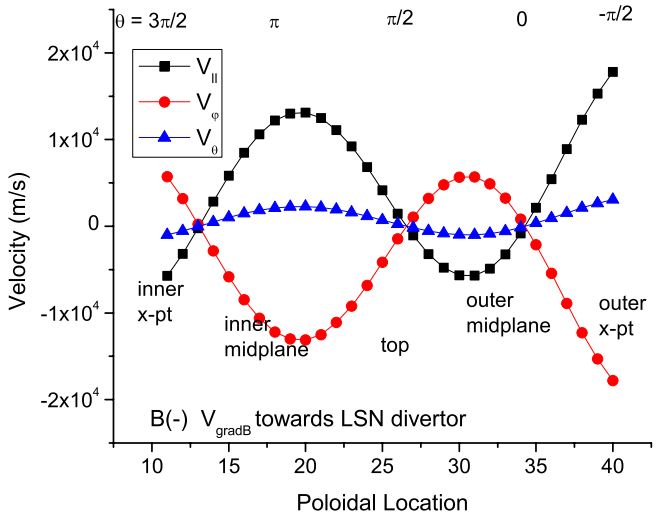

FIG. 4. (Color online) Velocities for (*B*−) case.

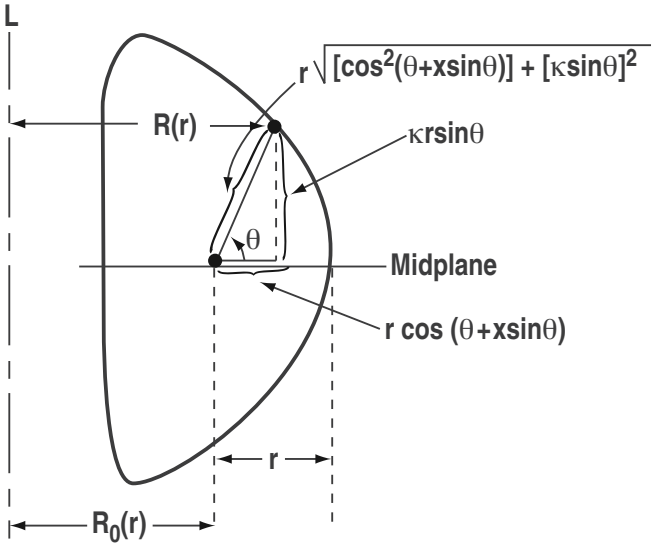

FIG. 5. Miller equilibrium parameters.

tation of this poloidal dependence. Miller *et al.*[10] derived analytical expressions for an equilibrium flux surface in a plasma, as shown in Fig. 5 with elongation κ, triangularity δ, and displaced centers $R_0(r)$, where r is the half diameter of the plasma along the midplane with center located at distance $R_0(r)$ from the toroidal center line. Note that the positive direction of the angle θ shown in Fig. 5 corresponds to the direction of B_θ produced by a plasma current out of the page (rather than into the page as in Fig. 2), i.e., a clockwise plasma current looking down on the tokamak. Thus, the positive sense of the angle θ used in describing the equilibrium geometry of Fig. 3 is upward at the outboard midplane, opposite to the positive sense of angle θ used in the rotation velocity and viscosity calculations described above. The angle θ defined in Fig. 3 is the angle θ indicated in Figs. 1, 2, and 4–7.

The R and Z coordinates of this plasma are described by

$$R(r) = R_0(r) + r\cos[\theta + x\sin\theta] \equiv R_0(r) + r\cos\xi,$$
$$Z(r) = \kappa r\sin\theta, \tag{3}$$

where $x \equiv \sin^{-1}\delta$. The poloidal magnetic field in such flux surface geometry is

$$RB_\theta = |\nabla\phi \times \nabla\psi| = \frac{\partial\psi}{\partial r}|\nabla r| = \frac{\partial\psi}{\partial r}\kappa^{-1}\Lambda(r,\theta)$$
$$\equiv \frac{\frac{\partial\psi}{\partial r}\kappa^{-1}[\sin^2(\theta + x\sin\theta)(1 + x\cos\theta)^2 + \kappa^2\cos^2\theta]^{1/2}}{\cos(x\sin\theta) + \frac{\partial R_0}{\partial r}\cos\theta + [s_\kappa - s_\delta\cos\theta + (1+s_\kappa)x\cos\theta]\sin\theta\sin(\theta + x\sin\theta)}, \tag{4}$$

where $s_\kappa = (r/\kappa)(\partial\kappa/\partial r)$ and $s_\delta = r(\partial\delta/\partial r)/\sqrt{(1-\delta^2)}$ account for the change in elongation and triangularity, respectively, with radial location.

The shifted circle model (which leads to the Shafranov shift) yields

$$\frac{\partial R_0}{\partial r} \equiv \Delta' = -\frac{r}{R_0}\left(\beta_\theta + \frac{1}{2}\ell_i\right). \tag{5}$$

Here $\beta_\theta = nT/B_\theta^2/2\mu_0$ and ℓ_i is the internal inductance.

The definition of the safety factor

$$q(r) = \frac{|B_{\phi 0}|}{2\pi}\oint\frac{d\ell_\theta}{RB_\theta} \tag{6}$$

and Eq. (4) can be used to evaluate

$$\frac{\partial\psi(r)}{\partial r} = \frac{|B_{\phi 0}|\kappa(r)}{2\pi q(r)}\oint\frac{d\ell_\theta}{\left[1 + \frac{r}{R_0(r)}\cos(\theta + x\sin\theta)\right]\Lambda(r,\theta)}. \tag{7}$$

The flux surface coordinate system is defined by the orthogonal coordinate directions (r,θ,ϕ) with length elements $d\ell_r = h_r dr$, $d\ell_\theta = h_\theta d\theta$, and $d\ell_\phi = h_\phi d\phi$. The coordinates θ and

Downloaded 06 Jan 2010 to 130.207.50.192. Redistribution subject to AIP license or copyright; see http://pop.aip.org/pop/copyright.jsp

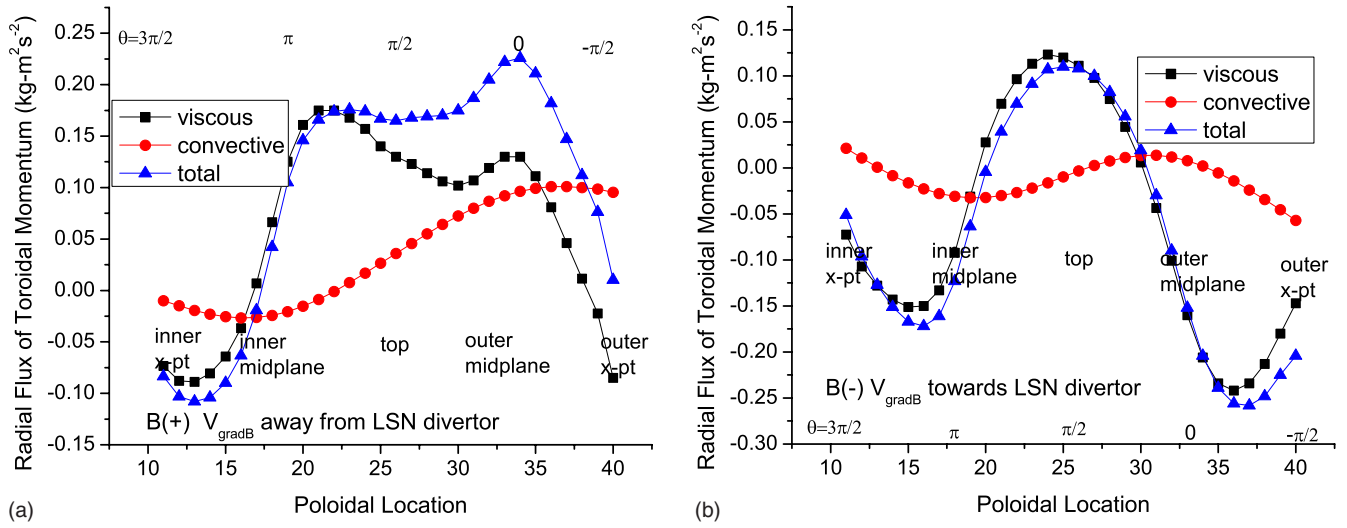

FIG. 6. (Color online) (a) Flux of toroidal momentum for (B+). (b) Flux of toroidal momentum for (B–).

ϕ lie in the flux surface and represent a poloidal anglelike variable θ shown in Fig. 1 and the toroidal angle ϕ, respectively. The r coordinate is normal to the flux surface. With the Miller equilibrium, the metric coefficients are

$$h_r = 1/|\nabla r(r,\theta)|,$$

$$h_\theta = r\sqrt{\cos^2(\theta + x\sin\theta) + \kappa^2 \sin^2\theta}, \tag{8}$$

$$h_\phi = R_0(r) + r\cos(\theta + x\sin\theta).$$

In this flux surface geometry the viscous fluxes of Eqs. (1) and (2) can be written as[11]

$$\Pi_{r\varphi} = -\eta_4\left\{\frac{\partial V_\varphi}{h_\theta \partial\theta} + \frac{V_\varphi r\sin(\theta + x\sin\theta)(1 + x\cos\theta)}{h_\theta[R_0 + r\cos(\theta + x\sin\theta)]}\right\} \tag{9}$$

and

$$\Pi_{r\theta} = \frac{1}{2}\left[\Pi_{r\varphi} - \eta_4\frac{\partial \ell n(|\nabla r|)}{h_\theta \partial\theta}\right]. \tag{10}$$

These two viscous fluxes have been evaluated using the calculated (V_φ, V_θ) θ-distributions along the separatrix shown in Figs. 3 and 4. The results of these calculations are plotted in Figs. 6 and 7. Also shown are the convective momentum fluxes discussed previously and the sum of the viscous and convective momentum fluxes crossing the separatrix.

From a comparison of Figs. 6(a) and 6(b), it can be seen that both the viscous and total calculated radial fluxes of toroidal momentum crossing the separatrix are more positive when B is parallel with the current (B+) than when B is antiparallel with the current (B–). The same general trend—more positive radial fluxes for (B+) than for (B–)—are displayed for the calculated radial fluxes of poloidal momentum in Figs. 7. The radial fluxes of poloidal momentum are generally smaller than the toroidal momentum fluxes by a factor

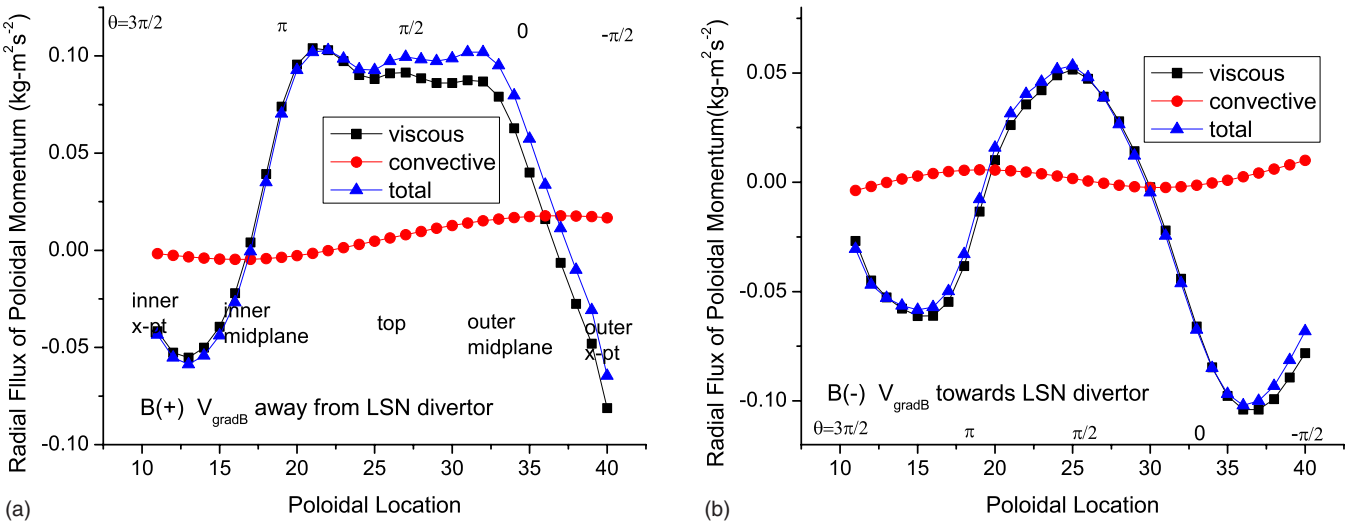

FIG. 7. (Color online) (a) Flux of poloidal momentum for (B+). (b) Flux of poloidal momentum for (B–).

Downloaded 06 Jan 2010 to 130.207.50.192. Redistribution subject to AIP license or copyright; see http://pop.aip.org/pop/copyright.jsp

of 2 or more. Since the radial momentum fluxes at the separatrix depend on the direction of the toroidal field, it is anticipated that the toroidal and poloidal rotation velocities within the edge pedestal will also depend on the direction of the toroidal field.

The magnitude of the effect of such radial momentum fluxes on the toroidal rotation within the edge pedestal can be roughly estimated by balancing the momentum deposition/loss in the pedestal due to the divergence of the viscous flux with the acceleration of deuterium ions, $d\Pi_{r\varphi}/dr \approx \mathrm{nm}\, dV_{\varphi}/dt$. Using the above results and typical parameters for DIII-D, an order of magnitude estimate for a representative value of the viscous flux $\Pi_{r\varphi} \approx 0.1$ kg m/s^2 and an assumed pedestal width of 10 cm for the momentum deposition/loss leads to a quite large toroidal acceleration $dV_{\varphi}/dt \sim 10^6$ m/s^2. A similar estimate results for poloidal acceleration driven by $\Pi_{r\theta}$.

The predominantly positive toroidal momentum fluxes shown in both of Fig. 6 would tend to drive a positive toroidal rotation in the edge pedestal. This result is suggestive of a cause for the observed corotation (i.e., in the direction of the plasma current) observed in C-MOD *H*-mode plasmas in the absence of external momentum input.[12] Of similar interest is the prediction of a viscous torque of poloidal momentum in the edge plasma driven by SOL flows. We plan to investigate these effects further.

IV. SUMMARY

The poloidal distribution of the deuterium parallel flow velocity along the separatrix was calculated for a model problem representative of a DIII-D *H*-mode discharge, based on divertor-SOL physics. This flow was then used to calculate the neoclassical radial viscous fluxes of toroidal and poloidal momentum just inside the separatrix in the edge pedestal, using an analytical representation of the elongated flux surface geometry and a Shafranov shift to provide a realistic evaluation of important poloidal dependences. The estimated effect of the parallel flows in the SOL on the rotation velocities in the edge pedestal is substantial and suggests a possible cause for the observed corotation in *H*-mode plasmas in the absence of external momentum input.

These results suggest that the parallel flows in the SOL, which are driven by particle outfluxes from the core plasma into the SOL and by SOL-divertor physics, may have a significant effect on toroidal (and poloidal) rotation velocities, hence on the structure of profiles, in the edge pedestal. They also suggest that these effects may depend on toroidal field direction (grad-B drift direction).

ACKNOWLEDGMENTS

This work was supported by the U. S. Department of Energy under Grant No. DE-FG02-00-ER54538 with the Georgia Tech Research Corporation.

[1] B. LaBombard, J. E. Rice, A. E. Hubbard, J. W. Hughes, M. Greenwal, F. S. Granetz, J. H. Irby, Y. Lin, B. Lipschultz, E. S. Marmar, K. Marr, D. Mossessian, R. Parker, W. Rowan, N. Smick, J. A. Snipes, J. L. Terry, S. M. Wolfe, S. J. Wukitch, and the Alcator C-MOD team, Phys. Plasmas **12**, 056111 (2005).
[2] M. Groth, G. D. Porter, J. A. Boedo, N. H. Brooks, R. C. Isler, W. P. West, B. D. Bray, M. E. Fenstermacher, R. J. Groebner, A. W. Leonard, R. A. Moyer, T. D. Rognlien, J. G. Watkins, and J. H. Yu, "Measurements and simulations of scrape-off layer flows in the DIII-D tokamak," J. Nucl. Mater. (to be published).
[3] A. Y. Aydemir, Phys. Plasmas **14**, 056118 (2007).
[4] W. M. Stacey, Phys. Plasmas **16**, 042502 (2009).
[5] W. M. Stacey, Phys. Plasmas **16**, 032506 (2009).
[6] W. M. Stacey and R. J. Groebner, Phys. Plasmas **12**, 042504 (2005).
[7] J. Luxon, Nucl. Fusion **42**, 614 (2002).
[8] W. M. Stacey, Phys. Plasmas **5**, 1015 (1998); **9**, 3673 (2002); Nucl. Fusion **40**, 965 (2000).
[9] W. M. Stacey and D. J. Sigmar, Phys. Fluids **28**, 2800 (1985).
[10] R. L. Miller, M. S. Chu, J. M. Greene, Y. R. Lin-Liu, and R. E. Waltz, Phys. Plasmas **5**, 973 (1998).
[11] W. M. Stacey and C. Bae, "Representation of the plasma fluid equations in Miller analytical flux surface coordinates," Phys. Plasmas (submitted).
[12] J. E. Rice, E. S. Marmar, P. T. Bonoli, R. S. Granetz, M. J. Greenwald, A. E. Hubbard, J. W. Hughes, I. H. Hutchinson, J. H. Irby, B. LaBombard, W. D. Lee, Y. Lin, D. Mossessian, J. A. Snipes, S. M. Wolfe, and S. Wukitch, Fusion Sci. Technol. **51**, 288 (2007).

Downloaded 06 Jan 2010 to 130.207.50.192. Redistribution subject to AIP license or copyright; see http://pop.aip.org/pop/copyright.jsp